Renormalization-group approach to multifractal structure of growth probability distribution in diffusion-limited aggregation

Takashi Nagatani
College of Engineering, Shizuoka University, Hamamatsu 432, Japan
(Received 29 June 1987)

The scaling structure of the growth probability distribution in the surface layer of the generalized diffusion-limited aggregation model (η model) is derived by making use of the real-space renormalization-group method. A conductance of the surface layer is defined and renormalized as the growth-bond conductance. The renormalization-group transformation equation is derived for the growth-bond conductance. The equation has a nontrivial solution which is a stable fixed point. The growth probability assigned to each growth bond is represented by a random multiplicative process of the cell's growth probabilities evaluated at the fixed point. A hierarchy of generalized dimensions $D(q)$ is calculated and the α-f spectrum is found for diffusion-limited-aggregation. The dependence of the α-f spectra is found on the parameter η describing the different dielectric breakdown models.

I. INTRODUCTION

Recently, there has been increasing interest in the problem of geometrical structure in diffusion-limited aggregation (DLA).[1-9] The structure of the aggregates strongly depends on the dynamics of the growth process. It is well known that they have a strong measure of self-similarity, which is characterized by the fractal dimensions D.[10] Several analytical attempts, including mean-field theories[11-13] and position-space renormalization-group methods,[14-17] have been made to derive the fractal dimension. It is clear, however, that an aggregate cannot be fully characterized by its fractal dimensionality. The essential properties of kinetic aggregation processes are described by the growth probability distribution for perimeter bonds (or sites) of these aggregating clusters.[18,19] Halsey *et al.*[18] and Amitrano *et al.*[19] calculated the growth probability distribution on the perimeter sites of the aggregates numerically and found a hierarchy of generalized dimensions $D(q)$. They introduced the α-f spectrum to describe the multifractal structure. Coniglio[20] proposed a mechanism which generates the multifractality, based on a multiplicative process[21] for the deterministic hierarchical model of the percolating cluster. Nagatani[22] presented a real-space renormalization-group (RG) method and found a random multiplicative process of the cell's growth probability under the RG transformation. The infinite exponents $D(q)$ and the α-f spectrum were first found from a standpoint of the RG.

In this paper we present an improved RG method for the multifractal structure in the DLA model. The RG method is developed to calculate the scaling structures in the generalized DLA model (η model). We derive the α-f spectra for the η model from the real-space RG method. We refer to the dielectric breakdown description of DLA. In general, aggregates grown on lattices are viewed as a system of superconductor–normal resistor networks for the dielectric breakdown models. The growth occurs on the perimeter of the aggregate. In these models the growth probability p_i at the growing perimeter bond i is given by $p_i \sim (E_i)^\eta$ where E_i is the local electric field at the growth bond. We merely solve an electrostatic problem for a superconducting cluster inside an infinite normal resistor network. We distinguish between three types of bonds on the lattice: (a) superconducting bonds, (b) growth bonds which are normal resistors at the perimeter of the aggregate, and (c) normal resistor bonds except for the growth bonds. For later convenience we summarily explain the RG method for DLA. Cover all the space of the square lattice by cells of edge b (scale factor), each containing $2b^2$ bonds. After a renormalization transformation these cells play the role of "renormalized" bonds. The dividing and rescaling of b $(=2,3,\frac{3}{2})$ cells for the DLA on the square lattice are illustrated in Figs. 1(a), 1(b), and 1(c). The cells on the left-hand side are renormalized to those on the right-hand side. The renormalized bonds are indicated by the double lines in each figure. The renormalized bonds are then classified into three types of bonds: (a) break bonds which construct the aggregate, (b) growth bonds which are on the perimeter of the aggregate and can be successively grown, and (c) unbroken bonds which surround the aggregate, except for the growth bonds. The renormalization procedure is illustrated in Fig. 2. The break, growth, and unbroken bonds are, respectively, indicated by the bold, wavy, and light lines. If the cell is spanned with the break bonds, then the renormalized bond is considered to be broken [Fig. 2(a)]. If the cell is not spanned with the break bonds and is a nearest neighbor to the cell with spanning cluster, then the cell is renormalized as a growth bond [Fig. 2(b)]. When the cell is constructed by unbroken bonds only and is not a nearest neighbor to the cells with spanning clusters, the cell is renormalized as an unbroken bond [Fig. 2(c)]. We consider the growth bonds

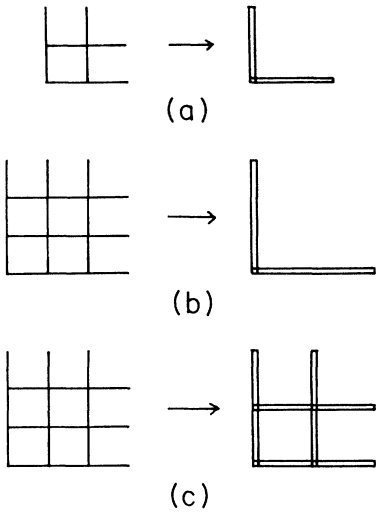

FIG. 1. Illustration of the dividing and rescaling of b $(=2,3,\frac{3}{2})$ cells for the DLA on the square lattice. (a) A $b=2$ cell, (b) a $b=3$ cell, (c) from a $b=3$ cell to a $b=2$ cell. The cell-to-cell transformation

construct the surface layer of the aggregates. Figure 3 shows an example of the renormalization of a part of the surface layer of an aggregate. The lattice on the left-hand side is renormalized to that on the right-hand side, according to the rules of renormalization. We define the conductance of the growth bonds as a conductance of the surface layer. We note that the nonlocal nature of the electric field is taken into account as the conductance of the growth bonds. We consider a renormalization of the conductance of the growth bonds. If a cell is renormalized as a growth bond, the cell's conductance σ_{n+1} is then represented by the conductance σ_n of the growth bond within the cell after the $(n+1)$th renormalization transformation:

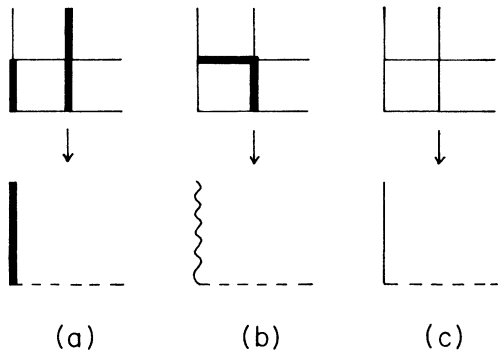

FIG. 2. Illustration of the renormalization of a $b=2$ cell for DLA. The renormalization procedure in the vertical direction is shown. There are three types of bond: break bonds indicated by bold lines, growth bonds indicated by wavy lines, and unbroken bonds indicated by light lines. Examples of the distinct configurations are shown in (a), (b), and (c), which are renormalized as break, growth, and unbroken bonds, respectively.

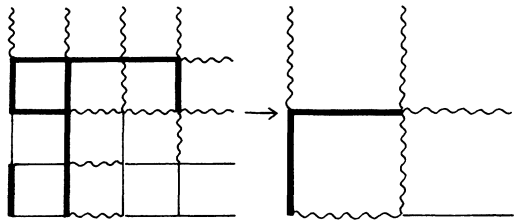

FIG. 3. An example of the renormalization of a part of the surface layer of an aggregate. The lattice on the left-hand side is renormalized to that on the right-hand side, according to the rules of renormalization.

$$\sigma_{n+1}=R(\sigma_n) . \tag{1}$$

The relationship (1) represents the renormalization-group equation. Figure 4 shows a schematic behavior of the renormalization function $\sigma'=R(\sigma)$. This has a nontrivial solution σ^* (>1). At the fixed point σ^* the derivative $dR/d\sigma$ has a positive value less than 1. The equation (1) has a stable fixed point. After many repeated renormalizations, the conductance of the growth bonds approaches the value σ^* at the fixed point. This represents a stable steady state. After renormalization, the growth probability $P_i(L)$ on any growth bond i is given by

$$P_i(L)=p_{\beta,i}P_\beta(L/b) , \tag{2}$$

where L represents the size of the system, b is the scale factor, and $p_{\beta,i}$ indicates the growth probability of the growth bond i within the cell β. The cell's growth probability $p_{\beta,i}$ is represented by a function of the conductance of the growth bonds. After many repeated renormalizations, the growth probability assigned to each growth bond is represented by a random multiplicative process of the cell's growth probabilities evaluated at the fixed point. In the limit of L sufficiently larger, an infinite hierarchy of generalized dimensions $D(q)$ is given by

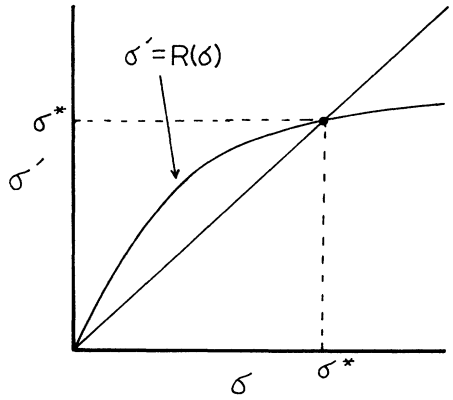

FIG. 4. A schematic behavior of the renormalization function $\sigma'=R(\sigma)$. This has a nontrivial solution σ^* (>1). At the fixed point σ^* the derivative $dR/d\sigma$ has a positive value less than 1. The fixed point is stable.

$$D(q)=-(q-1)^{-1}\ln\left\langle \sum_i p_{\alpha,i}^{*q} \right\rangle_c / \ln b \ , \tag{3}$$

where $\langle \cdots \rangle_c$ indicates the configurational average and $p_{\alpha,i}^{*}$ represent the cell's growth probability evaluated at the fixed point. The partition of $D(q)$ into a density of singularities $f(q)$ with singularity strength $\alpha(q)$ is introduced:

$$\begin{aligned} \alpha(q)&=d/dq[(q-1)D(q)] \ , \\ f(q)&=q\alpha(q)-(q-1)D(q) \ . \end{aligned} \tag{4}$$

The α-f spectrum is found.

We begin, in Sec. II, by applying the real-space renormalization-group method to the diffusion-limited aggregation on the square lattice. We refer to the dielectric breakdown description of DLA. We derive the scaling structure of the growth probability distribution on the surface layer of DLA from small-cell renormalization techniques. In Sec. III we derive the scaling structures for the generalized DLA (η model). The dependence of the α-f spectra is found on the parameter η describing the different dielectric breakdown models.

II. SMALL-CELL RENORMALIZATION FOR DLA

In this section we apply the real-space RG method to the self-similar structure of DLA. When DLA grows on the square lattice, the structure shows a crossover to an anisotropic shape on large length scales.[23–25] We define ξ_c as the crossover length. The self-similarity of DLA breaks down for large sizes of the order of ξ_c as well as for small sizes of the order of the distance a between nearest neighbors on the lattice. We apply the RG to DLA with the system length L smaller than the crossover length ξ_c as well as larger than a. In real-space renormalization, we replace a cell of bonds by a single superbond, provided that the linear dimension b of the cell is much smaller than ξ_c. The renormalized bonds are classified into three types of bonds: break, growth, and unbroken bonds. The growth probability distribution on the surface layer relates to the cell's growth probability and the conductance of growth bonds. We pay attention to the growth bonds. We consider configurations of the cell that it is possible to renormalize as the growth bond. We derive the cell's growth probability from the renormalization of the growth bond conductance. We find the generalized dimension $D(q)$ and the α-f spectrum.

A. The simplest cell (2×2 cell)

We start by partitioning the square lattice into 2×2 cells which cover the lattice [see Fig. 1(a)]. We give attention to the growth bonds which construct the surface layer of the aggregate. We consider the conductance of the cell that it is possible to renormalize as the growth bond. If one considers the renormalization in the vertical direction, we shall take periodic boundary conditions in lateral direction. The constant voltage is vertically applied [see Fig. 5(a)]. Figure 5(b) shows all configurations of the cell that it is possible to renormalize as the growth bond. Let us consider the

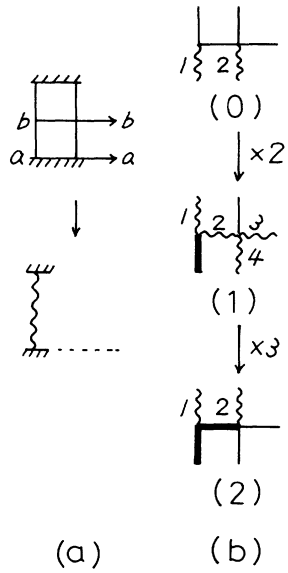

FIG. 5. (a) Boundary conditions in the renormalization in the vertical direction. The constant voltage is vertically applied. The periodic boundary condition is taken in lateral direction. (b) All distinct configurations of the 2×2 cell that it is possible to renormalize as the growth bond. The configuration (1) is constructed by adding a break bond onto the growth bond 1 or 2 in the configuration (0). In addition, by adding a break bond onto the growth bond 2, 3, or 4 in the configuration (1), the configuration (2) is constructed.

configurational probability C_α with which a particular configuration α appears. The distinct configurations are labeled by α ($\alpha=0,1,2$) in Fig. 5(b). The configuration (1) is constructed by adding a break bond to configuration (0). The probability with which a break bond adds onto growth bond 1 or 2 in configuration (0) is given by the growth probabilities $p_{0,1}$ or $p_{0,2}$ of the growth bonds 1 or 2 in the configuration (0). In addition, by adding a break bond to the configuration (1), the configuration (2) occurs. The configurational probabilities C_α are given by

$$\begin{aligned} C_1&=C_0(p_{0,1}+p_{0,2})=2C_0p_{0,1} \ , \\ C_2&=C_1(p_{1,2}+p_{1,3}+p_{1,4})=3C_1p_{1,2} \ , \end{aligned} \tag{5}$$

where $p_{0,1}=p_{0,2}$ and $p_{1,2}=p_{1,3}=p_{1,4}$. The configurational probability C_0 is determined from the normalization condition

$$\sum_\alpha C_\alpha = C_0+C_1+C_2=1 \ . \tag{6}$$

In general, the probability that a given growth-cluster configuration of n bonds occurs is given by the product of growth probabilities of adding a break bond at each step. The configurational probability C_α is determined by the growth probabilities $p_{\alpha,i}$ of the cells. The growth probability $p_{\alpha,i}$ on the growth bond i within the cell α is proportional to the local electric field E_i on the growth bond. Consider the electrostatic problem for cells which

can be renormalized as the growth bond. The electric fields on the growth bonds within a cell are determined by the conductance of growth bonds and the configuration of the cell. In the configuration labeled by α [see Fig. 5(b)], the growth probabilities $p_{\alpha,i}$ of growth bonds i are given by

$$\begin{aligned} &p_{0,1}=p_{0,2}=\tfrac{1}{2}\ , \\ &p_{1,1}=(1+3\sigma)/(4+3\sigma)\ , \\ &p_{1,2}=p_{1,3}=p_{1,4}=1/(4+3\sigma)\ , \\ &p_{2,1}=p_{2,2}=\tfrac{1}{2}\ , \end{aligned} \tag{7}$$

where the σ indicates the conductance of the growth bond, and the conductances of the break and unbroken bonds are, respectively, given by infinite value and unit value.

We consider the conductance σ_{n+1} of the cell renormalized as the growth bond at the $(n+1)$th renormalization stage [see Fig. 5(b)]. The conductance $\sigma_{\alpha,n+1}$ of the cell with configuration α is renormalized as follows:

$$\begin{aligned} &\sigma_{0,n+1}=2\sigma_n/(1+\sigma_n)\ , \\ &\sigma_{1,n+1}=\sigma_n+3\sigma_n/(1+3\sigma_n)\ , \\ &\sigma_{2,n+1}=2\sigma_n\ . \end{aligned} \tag{8}$$

The $(n+1)$th renormalized conductance σ_{n+1} of the growth bond will be assumed to be given by the most probable value[26]

$$\sigma_{n+1}=\exp(C_0\ln\sigma_{0,n+1}+C_1\ln\sigma_{1,n+1}+C_2\ln\sigma_{2,n+1})\ , \tag{9}$$

where C_α represents the probability of a particular configuration α. The relationships (8) and (9) present the renormalization-group equation $\sigma_{n+1}=R(\sigma_n)$. Equations (5)–(9) are simultaneously solved. We find a stable fixed point $\sigma^*=2.326$ from $\sigma^*=R(\sigma^*)$. At the fixed point, we evaluate the cell's growth probability $p^*_{\alpha,i}$ on the growth bond i within the cell α from Eq. (7). We calculate the generalized dimensions $D(q)$ from Eq. (3) where the configurational average is taken by using Eq. (5) evaluated at the fixed point. The exponents $D(q)$ are plotted as curve a in Fig. 7. The values of $D(q)$ are shown in Table I. One calculates the α-f spectrum via Eq. (4). We display the relation between α and f as curve a in Fig. 8.

B. 3×3 cell

We extend the renormalization transformation of the 2×2 cell to that of the 3×3 cell. Partition the square lattice into 3×3 cells which cover the lattice [see Fig. 1(b)]. We pay attention to the growth bonds. We consider configurations of the cell that it is possible to renormalize as the growth bond. When one performs the renormalization procedure of the cell in the vertical direction, the constant voltage is vertically applied and periodic boundary conditions are taken in the lateral direction. Figure 6 shows all configurations of the cell that it is possible to renormalize as the growth bond in the vertical direction. The distinct configurations are labeled by α (α=0,1,21,22,31,32,33,41,42,43,44,51,52,6) in Fig. 6. The configuration (1) is constructed by adding a break bond onto growth bonds 1, 2, or 3 in the configuration (0). In addition, by adding a break bond to the configuration (1), the configurations (21) and (22) occur where the configuration (21) is constructed by adding a break bond onto the growth bond 1 in the

TABLE I. Values of D_q for DLA obtained from the RG transformations shown in Figs. 1(a), 1(b), and 1(c).

	Fig. 1(a)	Fig. 1(b)	Fig. 1(c)
D_{-5}	2.947	4.654	7.572
D_{-4}	2.846	4.388	7.025
D_{-3}	2.695	3.990	6.204
D_{-2}	2.454	3.341	4.858
D_{-1}	2.058	2.303	2.722
D_0	1.526	1.482	1.406
D_1	1.096	1.095	1.093
D_2	0.934	0.956	0.992
D_3	0.845	0.863	0.892
D_4	0.792	0.802	0.821
D_5	0.752	0.759	0.771
D_6	0.721	0.726	0.736
D_∞	0.504	0.525	0.560

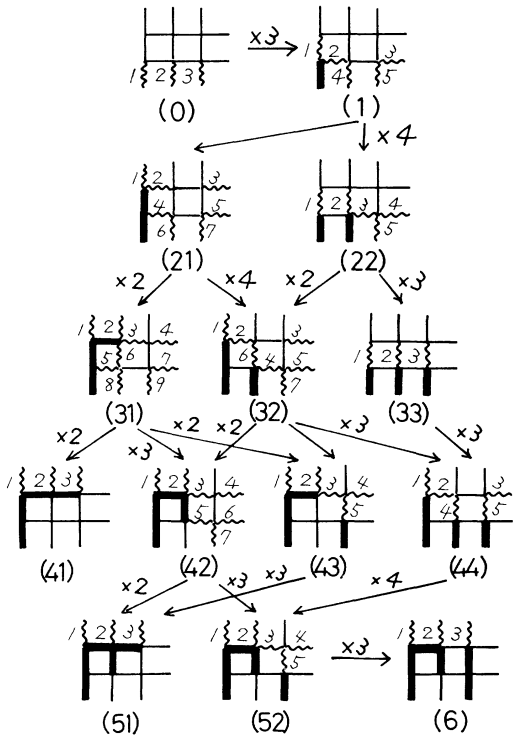

FIG. 6. Construction of the distinct configurations of the 3×3 cell that it is possible to renormalize as the growth bond. The distinct configurations are labeled by α (=0,1,21,22,31,32,33,41,42,43,44,51,52,6). An arrow from the configuration α to the configuration β indicates the construction of the configuration β by adding a break bond onto a growth bond in the configuration α.

configuration (1), and the configuration (22) is constructed by adding a break bond onto the growth bonds 2, 3, 4, and 5 in the configuration (1). The configurations (31) and (32) occur when a break bond is added to the configuration (21). When a break bond is added to the configuration (22), the configurations (32) or (33) appear. Here the configuration (31) is constructed by adding a break bond onto the growth bonds 2 or 3 in the configuration (21). The configuration (32) is constructed by adding a break bond into the growth bonds 4, 5, 6, and 7 in the configuration (21) or by adding a break bond onto the growth bonds 1 and 2 in the configuration (22). By applying this procedure repeatedly, one can count the distinct configurations. The configurational probability C_α with which the configuration α appears is given by

$$
\begin{aligned}
&C_1=3p_{0,1}C_0,\quad C_{21}=p_{1,1}C_1\ ,\\
&C_{22}=4p_{1,2}C_1,\quad C_{31}=2p_{21,2}C_{21}\ ,\\
&C_{32}=4p_{21,4}C_{21}+2p_{22,1}C_{22},\quad C_{33}=3p_{22,3}C_{22}\ ,\\
&C_{41}=2p_{31,3}C_{31},\quad C_{42}=3p_{31,5}C_{31}+2p_{32,2}C_{32}\ ,\\
&C_{43}=2p_{31,7}C_{31}+p_{32,3}C_{32},\quad C_{44}=3p_{32,4}C_{32}+3p_{33,1}C_{33}\ ,\\
&C_{51}=2p_{42,3}C_{42}+3p_{43,3}C_{43},\quad C_{52}=3p_{42,5}C_{42}+4p_{44,2}C_{44}\ ,\\
&C_6=3p_{52,3}C_{52}\ ,
\end{aligned}
\tag{10}
$$

where the $p_{\alpha,i}$ indicates the cell's growth probability on the bond i in the cell within the configuration α: For example, $p_{22,3}$ is the growth probability on the growth bond 3 in the configuration (22). The configurational probability C_0 is determined from the normalization condition

$$\sum_\alpha C_\alpha=C_0+C_1+C_{21}+\cdots+C_{52}+C_6=1\ .$$

The cell's growth probability $p_{\alpha,i}$ is proportional to the electric field E_i on the growth bond i. The electric fields on the growth bonds within a cell are determined by the conductance of growth bonds and the configuration of the cell. The nonlocal nature of the electric field is taken into account as the conductance of the growth bonds. In the configuration labeled by α [see Fig. 6], the cell's growth probabilities $p_{\alpha,i}$ of growth bonds i are given in the Appendix. At the $(n+1)$th renormalization stage, the conductance $\sigma_{\alpha,n+1}$ of the cell with the configuration α is renormalized as follows:

$$
\begin{aligned}
&\sigma_{0,n+1}=3\sigma_n/(1+2\sigma_n)\ ,\\
&\sigma_{1,n+1}=\sigma_n(10+7\sigma_n)/(2+8\sigma_n+3\sigma_n^2)\ ,\\
&\sigma_{21,n+1}=\sigma_n(7+9\sigma_n+2\sigma_n^2)/(1+5\sigma_n+2\sigma_n^2)\ ,\\
&\sigma_{22,n+1}=\sigma_n(20+33\sigma_n)/(4+21\sigma_n+12\sigma_n^2)\ ,\\
&\sigma_{31,n+1}=\sigma_n(9+52\sigma_n+68\sigma_n^2\\
&\qquad\qquad+24\sigma_n^3)/(1+15\sigma_n+28\sigma_n^2+12\sigma_n^3)\ ,\\
&\sigma_{32,n+1}=\sigma_n(21+64\sigma_n+38\sigma_n^2\\
&\qquad\qquad+6\sigma_n^3)/(3+21\sigma_n+26\sigma_n^2+6\sigma_n^3)\ ,\\
&\sigma_{33,n+1}=3\sigma_n/(1+\sigma_n)\ ,\\
&\sigma_{41,n+1}=3\sigma_n\ ,\\
&\sigma_{42,n+1}=\sigma_n(7+22\sigma_n+12\sigma_n^2)/(1+8\sigma_n+6\sigma_n^2)\ ,\\
&\sigma_{43,n+1}=2\sigma_n+3\sigma_n/(1+3\sigma_n)\ ,\\
&\sigma_{44,n+1}=\sigma_n+4\sigma_n/(1+2\sigma_n)\ ,\\
&\sigma_{51,n+1}=3\sigma_n\ ,\\
&\sigma_{52,n+1}=2\sigma_n+3\sigma_n/(1+3\sigma_n)\ ,\\
&\sigma_{6,n+1}=3\sigma_n\ .
\end{aligned}
\tag{11}
$$

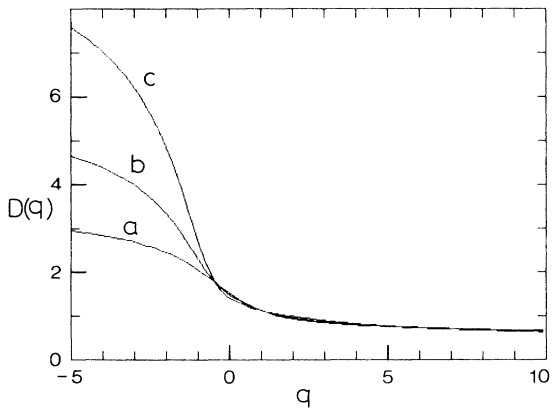

FIG. 7. The generalized dimension $D(q)$ of DLA obtained by the RG transformation of the three different cells; the curves a, b, and c indicate, respectively, the results of the 2×2 and 3×3 cells and the cell-to-cell transformation. The cell-to-cell RG transformation shows the successful improvement.

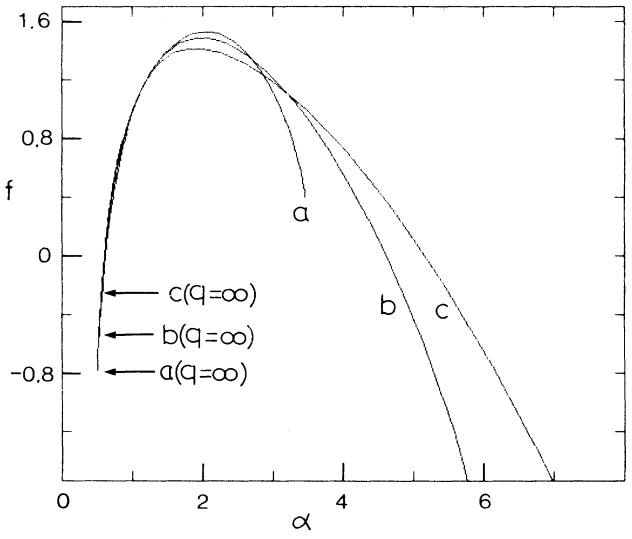

FIG. 8. The α-f spectra of DLA obtained by the RG transformation of the three different cells; the curves a, b, and c represent, respectively, the results of the 2×2 and 3×3 cells and the cell-to-cell transformation.

We assume that the $(n+1)$th renormalized conductance σ_{n+1} is given by the most probable value:

$$\sigma_{n+1}=\exp\left[\sum_{\alpha} C_{\alpha}\ln(\sigma_{\alpha,n+1})\right] . \tag{12}$$

The relationships (11) and (12) present the renormalization-group equation $\sigma_{n+1}=R(\sigma_n)$. Equations (10)–(12) and (A1)–(A14) are simultaneously solved. We find a stable fixed point $\sigma^*=2.213$ from $\sigma^*=R(\sigma^*)$. At the fixed point, we evaluate the cell's growth probabilities $p^*_{\alpha,i}$ from Eqs. (A1)–(A14). We calculate the generalized dimensions $D(q)$ from Eq. (3) where the configurational average is taken by using Eq. (10) evaluated at the fixed point. The exponents $D(q)$ are plotted as curve b in Fig. 7. The values of $D(q)$ are shown in Table I. The α-f spectrum is calculated from Eq. (4). The relation between α-f is displayed as curve b in Fig. 8.

C. Cell-to-cell transformation

Until now, we have considered the conventional RG approach of transforming from a system of cells to a new system of bonds. However, one can consider a transformation in which one passes from a system of cells of size b_1 to a system of cells of size b_2. Such a "cell-to-cell" transformation enables one to have a rescaling length b_1/b_2. We here consider the 3×3 cell to the 2×2 cell transformation. This cell-to-cell transformation is illustrated schematically in Fig. 1(c). We define $\sigma_{n+1}(b_j)=R(b_j;\sigma_n)$ to be the renormalized conductance of the growth bond for a cell of size b_j $(j=1,2)$. Then the renormalization-group equation is given by

$$R(b_2;\sigma_{n+1})=R(b_1;\sigma_n) , \tag{13}$$

where for $b_1=3$ and $b_2=2$ the $R(b_1;\sigma)$ and $R(b_2;\sigma)$ is, respectively, given by Eqs. (11) and (12) and by Eqs. (8) and (9). The fixed point is given by $R(b_2;\sigma^*)=R(b_1;\sigma^*)$. We define the cell's growth probability $p_{\alpha,i}(b_j)$ for a cell of size b_j $(j=1,2)$. The $p_{\alpha,i}(b_1)$ and $p_{\alpha,i}(b_2)$ are, respectively, given by Eqs. (A1)–(A14) and by Eq. (7). We obtain the exponents $D(q)$:

$$D(q)=-(q-1)^{-1}\ln\left[\left\langle\sum_i p^{*q}_{\alpha,i}(b_1)\right\rangle\Big/\left\langle\sum_j p^{*q}_{\beta,j}(b_2)\right\rangle\right]\Big/\ln(b_1/b_2) . \tag{14}$$

The exponents $D(q)$ are plotted as curve c in Fig. 7. The values of $D(q)$ are shown in Table I. The α-f spectrum is displayed as curve c in Fig. 8. This cell-to-cell RG transformation shows the successful improvement. These results of $D(q)$ and the α-f spectrum are close to the values obtained numerically by Amitrano *et al.*[19]

III. THE GENERALIZED DLA (η MODEL)

Niemeyer, Pietronero, and Wiesmann[27] proposed a very interesting dielectric breakdown model. In this model the growth probability P_i at the growing-perimeter bond i is given by $P_i\sim(E_i)^{\eta}$ where E_i is the local electric field on the perimeter bond i. When the parameter η equals 1, one recovers the DLA model. The structure of the aggregate changes drastically with varying η. This η model has a generalized form of the DLA. We apply the real-space RG method to the generalized DLA. The application procedure is straightforward. When we calculate the cell's growth probability $p_{\alpha,i}$, the relationship $p_{\alpha,i}\sim E_i$ is replaced by $p_{\alpha,i}\sim(E_i)^{\eta}$. We obtain the cell's growth probability for the η model.

TABLE II. Values of D_q for η model obtained from the RG transformation shown in Fig. 1(c).

	$\eta=0.4$	$\eta=0.8$	$\eta=1.2$
D_{-5}	3.015	6.086	9.011
D_{-4}	2.657	5.592	8.408
D_{-3}	2.215	4.856	7.502
D_{-2}	1.770	3.700	5.999
D_{-1}	1.473	2.179	3.346
D_0	1.369	1.404	1.399
D_1	1.331	1.360	1.048
D_2	1.222	1.079	0.898
D_3	1.215	1.006	0.778
D_4	1.193	0.944	0.703
D_5	1.171	0.897	0.656
D_6	1.151	0.861	0.626
D_∞	1.026	0.657	0.477

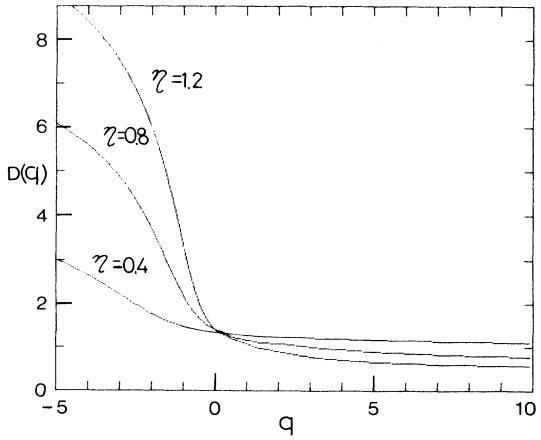

FIG. 9. The generalized dimension $D(q)$ of the generalized DLA (η model). The curves indicate, respectively, the results for $\eta=0.4$, 0.8, and 1.2.

We find the fixed point and the generalized dimensions $D(q)$ by using the cell-to-cell renormalization transformation presented by Sec. II C. The values of $D(q)$ for the η model are shown in Table II. For $\eta=0.4$, 0.8, and 1.2, the exponents $D(q)$ are plotted in Fig. 9. The α-f spectra are displayed in Fig. 10. As the parameter η increases, the α-f spectrum becomes a more smooth convex shape.

IV. SUMMARY

By making use of the real-space renormalization-group method, the set of generalized dimensions is derived in relation to the cluster structure of surface layers in diffusion-limited aggregation. The RG transformation equation is derived for the conductance of the cell which consists of the surface layer and is renormalized as the growth bond. The equation has a nontrivial solution which is a stable fixed point. The growth probability assigned to each growth bond is represented by a random multiplicative process of the cell's growth probabilities evaluated at the fixed point. A hierarchy of generalized dimensions $D(q)$ is calculated and the α-f spectra are found for the generalization DLA (η model).

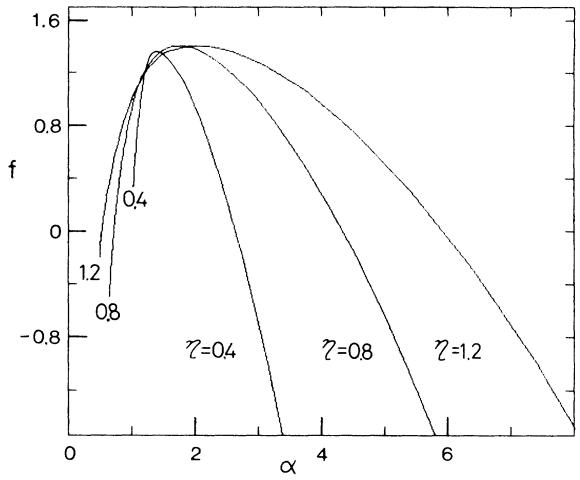

FIG. 10. The α-f spectra of the η model obtained from $D(q)$ of Fig. 9 for $\eta=0.4$, 0.8, and 1.2.

APPENDIX

In this appendix we present the cell's growth probabilities in the renormalization transformation of the 3×3 cell:

$$p_{0,1}=p_{0,2}=p_{0,3}=\tfrac{1}{3}\ ; \tag{A1}$$

$$p_{1,1}=(2+5\sigma)/(10+7\sigma)\ ,$$
$$p_{1,2}=p_{1,3}=p_{1,4}=p_{1,5}=(4+\sigma)/(20+14\sigma)\ ; \tag{A2}$$

$$p_{21,1}=(1+5\sigma+2\sigma^2)/(7+9\sigma+2\sigma^2)\ ,$$
$$p_{21,2}=p_{21,3}=(1+2\sigma)/(7+9\sigma+2\sigma^2)\ , \tag{A3}$$
$$p_{21,4}=p_{21,5}=p_{21,6}=p_{21,7}=1/(7+9\sigma+2\sigma^2)\ ;$$

$$p_{22,1}=p_{22,2}=(4+15\sigma)/(20+33\sigma)\ ,$$
$$p_{22,3}=p_{22,4}=p_{22,5}=(4+\sigma)/(20+33\sigma)\ ; \tag{A4}$$

$$p_{31,1}=p_{31,2}=(1+15\sigma+28\sigma^2+12\sigma^3)/(9+52\sigma+68\sigma^2+24\sigma^3)\ ,$$
$$p_{31,3}=p_{31,4}=(1+8\sigma+6\sigma^2)/(9+52\sigma+68\sigma^2+24\sigma^3)\ ,$$
$$p_{31,5}=p_{31,6}=p_{31,8}=1/(9+52\sigma+68\sigma^2+24\sigma^3)\ , \tag{A5}$$
$$p_{31,7}=p_{31,9}=(1+3\sigma)/(9+52\sigma+68\sigma^2+24\sigma^3)\ ;$$

$$p_{32,1}=(3+21\sigma+26\sigma^2+6\sigma^3)/(21+64\sigma+38\sigma^2+6\sigma^3)\ ,$$
$$p_{32,2}=p_{32,6}=(3+13\sigma+3\sigma^2)/(21+64\sigma+38\sigma^2+6\sigma^3)\ ,$$
$$p_{32,3}=(3+11\sigma+6\sigma^2)/(21+64\sigma+38\sigma^2+6\sigma^3)\ , \tag{A6}$$
$$p_{32,4}=p_{32,5}=p_{32,7}=(3+2\sigma)/(21+64\sigma+38\sigma^2+6\sigma^2)\ ;$$

$$p_{33,1}=p_{33,2}=p_{33,3}=\tfrac{1}{3}\ ; \tag{A7}$$

$$p_{41,1}=p_{41,2}=p_{41,3}=\tfrac{1}{3}\ ; \tag{A8}$$

$$p_{42,1}=p_{42,2}=(1+8\sigma+6\sigma^2)/(7+22\sigma+12\sigma^2)\ ,$$
$$p_{42,3}=p_{42,4}=(1+3\sigma)/(7+22\sigma+12\sigma^2)\ , \tag{A9}$$
$$p_{42,5}=p_{42,6}=p_{42,7}=1/(7+22\sigma+12\sigma^2)\ ;$$

$$p_{43,1}=p_{43,2}=(1+3\sigma)/(5+6\sigma)\ ,$$
$$p_{43,3}=p_{43,4}=p_{43,5}=1/(5+6\sigma)\ ; \tag{A10}$$

$$p_{44,1}=(1+2\sigma)/(5+2\sigma)\ ,$$
$$p_{44,2}=p_{44,3}=p_{44,4}=p_{44,5}=1/(5+2\sigma)\ ; \tag{A11}$$

$$p_{51,1}=p_{51,2}=p_{51,3}=\tfrac{1}{3}\ ; \tag{A12}$$

$$p_{52,1}=p_{52,2}=(1+3\sigma)/(5+6\sigma)\ ,$$
$$p_{52,3}=p_{52,4}=p_{52,5}=1/(5+6\sigma)\ ; \tag{A13}$$

$$p_{6,1}=p_{6,2}=p_{6,3}=\tfrac{1}{3}\ . \tag{A14}$$

[1]T. A. Witten and L. M. Sander, Phys. Rev. Lett. **47**, 1400 (1981).
[2]P. Meakin, Phys. Rev. A **27**, 1495 (1983).
[3]*Kinetics of Aggregation and Gelation*, edited by F. Family and D. P. Landau (North-Holland, Amsterdam, 1984).
[4]*On Growth and Form*, edited by H. E. Stanley and N. Ostrowsky (Nijhoff, The Hague, 1985).
[5]*Fractals in Physics*, edited by L. Pietronero and E. Tosatti (North-Holland, Amsterdam, 1986).
[6]*Scaling Phenomena in Disordered Systems*, edited by R. Pynn

and A. Skjeltorp (Plenum, New York, 1985).
[7]*Statistical Physics,* edited by H. E. Stanley (North-Holland, Amsterdam, 1986).
[8]P. Meakin, H. E. Stanley, A. Coniglio, and T. A. Witten, Phys. Rev. A **32**, 2364 (1985); **34**, 3325 (1986).
[9]P. Meakin, Phys. Rev. A **35**, 2234 (1987).
[10]B. B. Mandelbrot, *The Fractal Geometry of Nature* (Freeman, San Francisco, 1982).
[11]M. Muthukumar, Phys. Rev. Lett. **50**, 839 (1983).
[12]M. Tokuyama and K. Kawasaki, Phys. Lett. **100A**, 337 (1984).
[13]M. Matsushita, K. Honda, H. Toyoki, Y. Hayakawa, and H. Kondoh, J. Phys. Soc. Jpn. **55**, 2618 (1986).
[14]H. Gould, F. Family, and H. E. Stanley, Phys. Rev. Lett. **50**, 696 (1983).
[15]G. E. Green, J. Phys. A **17**, L437 (1984).
[16]H. Nakanishi and F. Family, Phys. Rev. A **32**, 3606 (1985).
[17]M. Kolb, J. Phys. A **20**, L285 (1987).
[18]T. C. Halsey, P. Meakin, and I. Procaccia, Phys. Rev. Lett. **56**, 854 (1986).
[19]C. Amitrano, A. Coniglio, and F. di Liberto, Phys. Rev. Lett. **57**, 1016 (1986).
[20]A. Coniglio, in *Statistical Physics,* edited by H. E. Stanley (North-Holland, Amsterdam, 1986), p. 51.
[21]L. Pietronero and A. P. Siebesma, Phys. Rev. Lett. **57**, 1098 (1986).
[22]T. Nagatani, J. Phys. A **20**, L381 (1987).
[23]P. Meakin, in *On Growth and Form,* edited by H. E. Stanely and N. Ostrowsky (Nijhoff, The Hague, 1985), p. 11.
[24]F. Family, T. Vicsek, and B. Taggett, J. Phys. A **19**, L727 (1986).
[25]R. C. Ball, in *Statistical Physics,* edited by H. E. Stanley (North-Holland, Amsterdam, 1986), p. 62.
[26]H. Furukawa, Prog. Theor. Phys. **73**, 586 (1985).
[27]L. Niemeyer, L. Pietronero, and H. J. Wiesmann, Phys. Rev. Lett. **52**, 1033 (1984).